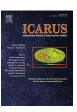


#### Contents lists available at ScienceDirect

### **Icarus**

journal homepage: www.elsevier.com/locate/icarus



# Horizontal and vertical structures of Jovian infrared aurora: Observation using Subaru IRCS with adaptive optics



Hajime Kita<sup>a,\*</sup>, Shota Fujisawa<sup>a</sup>, Chihiro Tao<sup>b</sup>, Masato Kagitani<sup>c</sup>, Takeshi Sakanoi<sup>c</sup>, Yasumasa Kasaba<sup>a</sup>

- <sup>a</sup> Department of Geophysics, Tohoku University, Sendai, Japan
- <sup>b</sup> National Institute of Information and Communications Technology, Koganei, Japan
- <sup>c</sup> Planetary Plasma and Atmospheric Research Center, Tohoku University, Sendai, Japan

#### ARTICLE INFO

#### Article history: Received 18 September 2017 Revised 15 April 2018 Accepted 1 May 2018 Available online 31 May 2018

Keywords: Jupiter Atmosphere Infrared aurora

#### ABSTRACT

We observed Jupiter's infrared aurora using the Subaru Infrared Camera and Spectrometer (IRCS) with adaptive optics, in order to compare horizontal and vertical emission profiles among H<sub>3</sub><sup>+</sup> fundamental, H<sub>3</sub><sup>+</sup> overtone, and H<sub>2</sub> emissions. The fundamental and overtone lines show similar horizontal distributions around the main auroral oval for both hemispheres. There is no correlation between the fundamental lines and temperature; however, a correlation seems to exist for the overtone lines. Although both the fundamental and overtone lines are related to electron precipitation, there are differences in the precipitating electron energies that influence the emissions, because of their different emission altitudes. In addition, the morphological difference between the H<sub>2</sub> and H<sub>3</sub>+ emission structures is significant. That is, the intensity of the  $H_3^+$  emission is enhanced around the main oval, but that of the  $H_2$  emission is not. The peak altitudes of the  $H_3^+$  fundamental,  $H_3^+$  overtone, and  $H_2$  are 650, 870, and 830km for the north and 700, 910, and 950km for the south, with the uncertainties of approximately 100km. This finding, that the fundamental emission peak altitude is found to be lower than those of the overtone and H<sub>2</sub> emissions, is consistent with the theoretical models and derived temperatures for the emission peak altitude. We also find similar peak altitudes for the H<sub>2</sub> and H<sub>3</sub><sup>+</sup> overtone emissions. This is in accordance with previous observations, which have revealed that the altitude of H<sub>2</sub> is higher than the model-based expectation. Collisional de-excitation of H<sub>2</sub> can dominate at lower altitudes, which might explain the higher emission peak altitude compared to that of the model.

© 2018 Elsevier Inc. All rights reserved.

#### 1. Introduction

Jupiter exhibits the strongest magnetospheric activity in the solar system. The Jovian magnetosphere, ionosphere, and thermosphere (MIT) are coupled electromagnetically, and strong auroral emission is consistently observed as a result. The MIT coupling current system, which flows outward in the magnetosphere and equatorward in the ionosphere, generates energy transfer from the upper atmosphere to the magnetosphere. The ionospheric current and vertical magnetic field accelerate plasma in the ionosphere in a sub-rotational direction, whereas the plasma in the magnetosphere is accelerated towards co-rotation. In addition, the magnetospheric energy returns to the upper atmosphere in the form of electrical current and energetic electrons precipitating along the field line.

The auroral region can be observed through the ultraviolet (UV) aurora, which is comprised of H and H2 emissions excited by the impacts of energetic electrons, and through the infrared (IR) aurora, which consists of thermally excited H<sub>3</sub><sup>+</sup> and H<sub>2</sub> emissions. The IR auroral emission intensities reflect the density and temperature of the neutral gases and plasma. The H<sub>3</sub><sup>+</sup> IR aurora is observed in the K- ( $\sim 2 \mu m$ ) and L-bands ( $\sim 4 \mu m$ ). H<sub>3</sub><sup>+</sup> is generated through interactions between atmospheric H2 and either precipitating electrons or solar extreme ultraviolet (EUV) radiation. Because H<sub>3</sub><sup>+</sup> has no permanent dipole moment, it has no pure rotational transitions at radio wavelength and exhibits vibrational and rotational-vibrational emissions in the IR range. The main emission modes are fundamental ( $\nu_2 = 1 \rightarrow 0$ ) and overtone ( $\nu_2 = 2 \rightarrow 0$ ), and their hotband counterparts ( $v_2 = 2 \rightarrow 1$  and  $v_2 = 3 \rightarrow 1$ ). H<sub>2</sub> is the dominant component of the Jovian atmosphere. The H<sub>2</sub> emission lines observed at the same wavelengths as this H<sub>3</sub>+ emission are quadrupole rotation-vibrational transitions in the K-band at approximately 2 µm. As the Einstein A-coefficient of H<sub>2</sub> emission is small (of the order of  $10^{-7} - 10^{-6}$  s<sup>-1</sup>), the emission

<sup>\*</sup> Corresponding author. E-mail address: kita@pat.gp.tohoku.ac.jp (H. Kita).

de-excitation timescale is larger than that of collisional de-excitation (the lifetime of the  $\nu\!=\!1$  level can be considerably shorter than  $10^4$  s (Cravens, 1987)). Therefore, the  $H_2$  emission intensity reflects the background kinetic temperature.

Horizontal and vertical distributions of  $\rm H_3^+$  and  $\rm H_2$  emissions have been investigated by many groups. The Jovian aurora mainly consists of three components; main oval, inner emission (polar emission) which is inside of the main oval, and outer emission (equatorward emission) which is outside of the main emission (Grodent et al., 2003; Grodent, 2015). The comparison between  $\rm H_3^+$  fundamental emission and UV aurora has been made by using the dataset obtained from HST and Infrared Telescope Facility (Clarke et al., 2004; Radioti et al., 2013). The morphology of the main oval was similar in both wavelength, but the polar region appeared to be quite different. Stallard et al. (2016) showed that the difference in the polar region could be explained by the difference in the timescale of the emission. They demonstrated that the averaged UV images over the timescale of an  $\rm H_3^+$  lifetime had a similar structure with the  $\rm H_3^+$  aurora around the polar region.

Raynaud et al. (2004) found the differences between the horizontal emission distributions of the  ${\rm H_3}^+$  R(7,7) overtone and  ${\rm H_2}$ S(1) lines in the northern polar region. The H<sub>3</sub><sup>+</sup> emission peak is located at 67°N latitude, System III longitude 150°  $\lambda_{III}$ , whereas that of  $H_2$  is at approximately 70°N 220°  $\lambda_{III}.$  The main oval cannot be identified. In contrast, the emission distribution in the southern polar region is spatially blurred, and both H<sub>2</sub> and H<sub>3</sub><sup>+</sup> emission maxima are present in the vicinity of  $60^{\circ}$ S,  $30-60^{\circ}$  $\lambda_{III}$ . Raynaud et al. (2004) also derived the  $H_3^+$  temperature at the northern pole from the observed spectrum and found that the emission peak region corresponds to the region in which the temperature is higher ( $\sim$ 1,175K) than that of the surroundings (~1,000K). Moreover, Chaufray et al. (2011) suggested that the difference in wind velocity between H<sub>3</sub>+ and H<sub>2</sub> is due to the difference in emission altitude, which may also explain the morphological difference.

Most auroral vertical structures are studied through theoretical analysis. Previously, Grodent et al. (2001) developed a onedimensional (1-D) model that couples a two-stream electron transport model of energy deposition with a 1-D thermal conduction model incorporating particle heating and cooling. However, the altitude profile of IR auroral emission is not realized under the Local Thermodynamic Equilibrium (LTE) condition (Kim et al., 1992). Subsequently, Melin et al. (2005) improved the model of Grodent et al. (2001) including this non-LTE effect. The improved model showed that, under non-LTE conditions, radiative de-excitation occurs on a shorter timescale than collisional deexcitation, and the populations of the excited states are lower than for the LTE case. The overtone emission peak altitudes decrease from  $\sim$ 1,500km under LTE to  $\sim$ 1,000km under non-LTE, but the fundamental emission peak altitudes are 500 – 600km under both conditions. Melin et al. (2005) also showed that the peak emission altitude of H<sub>3</sub><sup>+</sup> overtone emission can be 500–1,000km higher than that of H<sub>3</sub><sup>+</sup> fundamental emission. Note that the vertical density profiles of  $H_2$  ( $\nu = 1$ ) have been theoretically analyzed, based on the vibrational excitations of H2 molecules by solar EUV excitations, direct electron impact excitations, dissociative recombination of H<sub>3</sub>+, and excitation of the Lyman and Werner bands (Cravens, 1987; Kim, 1988; Kim et al., 1992). Vibrationally excited H<sub>2</sub> can react with either H2 or H via vibration-translation interchange collisions or vibration-vibration interchange collisions with other H<sub>2</sub> molecules. Assuming this behavior, the density peak of solar-EUVexcited  $H_2$  v = 1 is  $\sim 600 - 700$ km. For excitation by precipitated electrons with energies of 1, 10, and 100 keV, the density peaks are  $\sim$ 750,  $\sim$ 500, and  $\sim$ 300km, respectively (Cravens, 1987; Kim, 1988; Kim et al., 1992). These results suggest that the peak H<sub>2</sub> emission altitude may reflect the energy of the precipitating electrons above the main oval

The above emission altitudes are not only affected by the precipitating electron energy (Tao et al., 2011), but also by the vertical temperature profiles. The temperature derived by integrating the  $\rm H_3^+$  fundamental emission into the main oval is  $900-1,100\rm K$  (Grodent et al., 2001; Lystrup et al., 2008; Miller et al., 1990). For  $\rm H_3^+$  overtone emission, the derived temperatures for data averaged over the northern auroral region are 1,100K (vibration-rotational temperature; Miller et al. (1990)), 1,170K (rotational temperature, Raynaud et al. (2004)), and 960K (vibrational temperature, Raynaud et al. (2004)). The overtone temperatures are slightly higher than the fundamental temperature, which supports the finding that the peak altitude of the  $\rm H_3^+$  overtone emission is higher than that of the  $\rm H_3^+$  fundamental emission.

Under these circumstances, direct measurements of the peak altitudes of the  $\rm H_3^+$  fundamental,  $\rm H_3^+$  overtone, and  $\rm H_2$  emissions are necessary to confirm the vertical structure predicted by the established models. A direct comparison of the IR  $\rm H_2$  and  $\rm H_3^+$  overtone emission peak altitudes of the northern pole has been performed based on observation conducted using the Infrared Camera and Spectrometer (IRCS) on the Subaru telescope with adaptive optics (Uno et al., 2014). The results show that the differences in emission peak altitude among the IR  $\rm H_2$  and overtone emissions are small. This finding contradicts the expectation of Chaufray et al. (2011), which is based on the velocity difference between the IR  $\rm H_2$  and  $\rm H_3^+$  overtone emissions.

In this paper, we confirm the results described in Uno et al. (2014) and perform a comparison of the horizontal and vertical profiles of the H<sub>3</sub><sup>+</sup> fundamental and overtone emission lines. We also investigate the differences in the horizontal and vertical profiles of the H<sub>2</sub> and H<sub>3</sub><sup>+</sup> emissions in both the northern and southern polar regions. The horizontal temperature profiles of H<sub>2</sub> and H<sub>3</sub><sup>+</sup> are compared with their horizontal and vertical emissivity profiles. By examining these differences, we investigate the responses of the IR  $\mathrm{H_2}$  and  $\mathrm{H_3}^+$  emissions to the precipitating electrons, as suggested by Tao et al. (2011). H<sub>3</sub>+is sensitive to the flux and energy of the precipitation electrons, and this is especially apparent in the H<sub>3</sub><sup>+</sup> fundamental emissions. The H<sub>3</sub><sup>+</sup> overtone emissions can have higher sensitivity to surrounding temperatures; however, this behavior depends on the strength of the non-LTE effect. The H<sub>2</sub> density is independent of the electrons, but the vibrational excitation itself can be affected. These differences in the emission mechanisms could appear in the horizontal and vertical distributions of the IR emissions.

#### 2. Observation

We made observations of Jupiter's auroral region using the IRCS instrument attached to the Subaru 8.2m telescope at Mauna Kea, Hawaii, on Jan. 31, 2015. The overnight weather was good on that date. The diameter of the Jovian disk was 45.3 arcsec.

The cross-dispersed echelle spectrometer of the IRCS covers  $1-5\,\mu m$ . The slit (length: 5.17 arcsec, width: 0.27 arcsec) was set parallel to the Jovian rotational axis. The spectral resolution is  $R \sim 10,000$ . The IRCS is equipped with a  $1,024 \times 1,024$  pixel ALADDIN III InSb array detector with a pixel scale of 0.055 arcsec  $\times 0.068$  arcsec. In this study, we alternated between two wavebands, the K-(1.95–2.41  $\mu$ m) and L-bands (3.23–4.01  $\mu$ m). The L-band includes the  $H_3^+$  fundamental emission lines ( $v=1\rightarrow 0$ ) and the K-band includes both the  $H_3^+$  overtone ( $v=2\rightarrow 0$ ) and  $H_2$  emission lines. The strong methane absorption at the L-band effectively masks the thermal emissions and scattered sunlight from deeper levels in the atmosphere, which is known as haze. Each observation was conducted in an object-sky-object sequence. The integration time for the K-band spectrum was 150 sec  $\times$  1, and that for the L-band

## Download English Version:

# https://daneshyari.com/en/article/8133844

Download Persian Version:

https://daneshyari.com/article/8133844

<u>Daneshyari.com</u>